ported transmission among populations outside the major urban centers where the disease is currently believed to be concentrated.

Methodological issues qualify the GSS findings. The sample size is small and thus our estimates are imprecise. Larger samples would permit close inspection of the distribution of cases across geographic regions and facilitate multivariate analysis. With more details about the persons identified with AIDS, we could have avoided inferring the geographic location of the person with AIDS, for instance. More methodologically oriented network studies would permit us to estimate the size of personal acquaintance networks, knowledge of particular attributes of acquaintances, and effects of network density on accuracy of reports. More generally, we need a more accurate view of the social epidemiology of AIDS; for without it, public health measures may be misdirected in audience, geography, and timing.

REFERENCES AND NOTES

1. J. W. Curran *et al.*, *Science* **239**, 610 (1988).
2. Institute of Medicine, *Confronting AIDS, Directions for Public Health, Health Care, and Research* (National Academy Press, Washington, DC, 1986); C. F. Turner, H. G. Miller, L. E. Moses, Eds., *AIDS: Sexual Behavior and Intravenous Drug Use* (National Academy Press, Washington, DC, 1989).
3. R. Shilts, *And the Band Played On: Politics, People, and the AIDS Epidemic* (St. Martin's Press, New York, 1987); E. O. Laumann and D. Knoke, *The Organizational State: Social Choice in National Policy Domains* (Univ. of Wisconsin Press, Madison, 1987).
4. T. J. Dondero, M. Pappaioanou, J. W. Curran, *Public Health Rep.* **103**, 213 (1988).
5. E. O. Laumann, *Bonds of Pluralism* (Wiley, New York, 1973); J. C. Mitchell, *Social Networks in Urban Situations* (Manchester Univ. Press, Manchester, England, 1969), pp. 1–50; P. Holland and S. Leinhardt, *Perspectives on Social Network Research* (Academic Press, New York, 1979); C. Fischer, *To Dwell Among Friends* (Univ. of Chicago Press, Chicago, 1982); R. S. Burt, *Annu. Rev. Sociol.* 6, 79 (1980); ——— and M. Minor, *Applied Network Analysis* (Sage, Beverly Hills, CA, 1983); S. Berkowitz, *An Introduction to Structural Analysis: The Network Approach to Social Research* (Butterworths, Toronto, 1982).
6. J. Boissevain, *Friends of Friends: Networks, Manipulators, and Coalitions* (Blackwell, Oxford, 1974); I. Pool and M. Kochen, *Soc. Netw.* **1**, 5 (1978); L. C. Freeman and C. R. Thompson, in *The Small World*, M. Kochen, Ed. (Ablex, Norwood, NJ, in press).
7. H. R. Bernard, E. Johnsen, P. Killworth, "Estimating the size of hard-to-count populations" (grant proposal to the National Science Foundation, Washington, DC, 1988).
8. See also S. Sudman and G. Kalton, *Annu. Rev. Sociol.* **12**, 401 (1986); M. G. Sirken, *J. Am. Stat. Assoc.* **65**, 257 (1970); O. Frank. *Soc. Netw.* **1**, 91 (1978); S. Sudman *et al.*, *Science* **240**, 991 (1988).
9. National Opinion Research Center, *1988 General Social Survey*, J. A. Davis and T. W. Smith, principal investigators (Roper Center for Public Opinion Research, Storrs, CT).
10. Bureau of the Census, 1980 Census of Population, *General Population Characteristics*, part 1, *United States Summary* (Government Printing Office, Washington, DC, 1983); Current Population Reports, Series P-25, No. 1024, *State Population and Household Estimates, with Age, Sex, and Components of Change: 1981–87* (Government Printing Office, Washington, DC, 1988).
11. T. W. Smith and R. Fujimoto, *Annotated Bibliography of Papers Using the General Social Survey* (National Opinion Research Center, Chicago, ed. 6, 1986).
12. Federal Bureau of Investigation, *Uniform Crime Reports for the United States* (Department of Justice, Government Printing Office, Washington, DC, 1986).
13. National Center for Health Statistics, *Vital Statistics of the United States, 1985*, vol. II, *Mortality*, part B (Public Health Service, Government Printing Office, Washington, DC, 1987).
14. There is an extensive amount of literature in which the validity and accuracy of the official statistics on homicide and other criminal behavior are debated; however, most researchers agree that homicide is the most reliably reported of the Federal Bureau of Investigation's index of seven serious crimes. E. Sutherland and D. Cressey, *Criminology* (Lippincott, Chicago, 1978); G. Nettler, *Explaining Crime* (McGraw-Hill, New York, 1978); W. Gove, M. Hughes, M. Geerken, *Criminology* **23**, 451 (1985).
15. One hundred and fifty-six respondents knew one or more victims of homicide in the last 12 months (59 of these knew two or more). These 156 respondents were then asked to describe the victim whom they knew best. Because we tried to characterize all the victims of homicide known to respondents and not just the first victim mentioned, we report the total number of victims known in certain categories.
16. Centers for Disease Control, *AIDS Weekly Surveillance Rep.* (CDC, Atlanta, GA, 7 March 1988).
17. *Ibid.*, 16 May 1988.
18. It would be desirable to construct confidence intervals to assess the statistical significance of observed differences. It is not at all clear to us what sampling theory would be appropriate for the case in hand because we are not dealing with a "standard" problem in estimation from a well-defined population. We thus chose not to try to make such estimates because they are likely to be misleading or wrong.
19. There are a number of surveys that have asked whether respondents knew someone with AIDS. One such study was a telephone survey with random digit dialing done in Chicago from April to July 1987 [see D. G. Ostrow, S. Michaels, G. A. Albrecht, "Information and misinformation: The state of knowledge, attitudes and beliefs about AIDS in the Chicago metropolitan area general population" (preliminary report to the Chicago Department of Health's Comprehensive AIDS Prevention Education Program, Chicago, 1988)]. We compared the results from this telephone survey to the official reports on AIDS cases collected by the Chicago Department of Health. The result is strikingly similar to the national comparison: the survey data indicate a higher percentage of white cases than the official statistics (approximately 68 versus 58%) and a lower percentage of black cases (18 versus 33%).
20. M. Wolfgang, *Patterns of Criminal Homicide* (Univ. of Pennsylvania Press, Philadelphia, 1958); G. Braucht *et al.*, *Psychol. Bull.* **87**, 309 (1980); G. Nettler, *Killing One Another* (Anderson, Cincinnati, 1982).
21. *CDC Surveillance Report* (CDC, Atlanta, GA, 23 January 1989).

22. We gratefully acknowledge the helpful comments and suggestions of N. Bradburn, P. E. Converse, W. Coppelson, S. Hellman, R. L. Berkelman, J. Joseph, E. Kitagawa, R. Leo, M. Morris, S. H. Preston, M. Siegler, and T. W. Smith. The GSS is funded by NSF; the 1988 questions pertaining to sexual behavior and acquaintance with AIDS and homicide victims were funded by the National Opinion Research Center (NORC). Partial support for this research was provided by NSF through the National Data Program for the Social Sciences, NORC, and the National Institute of Child Health and Human Development (contract NO1-HD-8-2907).

14 November 1988; accepted 28 March 1989

Localization and Mobility of ω-Conotoxin–Sensitive Ca^{2+} Channels in Hippocampal CA1 Neurons

OWEN T. JONES, DIANA L. KUNZE, KIMON J. ANGELIDES*

Voltage-dependent Ca^{2+} channels (VDCCs) are modulators of synaptic plasticity, oscillatory behavior, and rhythmic firing in brain regions such as the hippocampus. The distribution and lateral mobility of VDCCs on CA1 hippocampal neurons have been determined with biologically active fluorescent and biotinylated derivatives of the selective probe ω-conotoxin in conjunction with circular dityndallism, digital fluorescence imaging, and photobleach recovery microscopy. On noninnervated cell bodies, VDCCs were found to be organized in multiple clusters, whereas after innervation the VDCCs were concentrated and immobilized at synaptic contact sites. On dendrites, VDCC distribution was punctate and was interrupted by extensive bare regions or abruptly terminated. More than 85% of the dendritic VDCCs were found to be immobile by fluorescence photobleach recovery. Thus, before synaptic contact, specific mechanisms target, segregate, and immobilize VDCCs to neuronal cell bodies and to specialized dendritic sites. Regulation of this distribution may be critical in determining the firing activity and integrative properties of hippocampal CA1 neurons.

THE INFLUX OF Ca^{2+} THROUGH voltage-dependent calcium channels (VDCCs) is important in the modulation of neuronal function (*1*). These Ca^{2+} influxes are often localized to discrete regions of the neuron (*2*) and are associated with regulation of neurotransmitter release (*3*), activation of Ca^{2+}-dependent enzymes (*4*), changes in neuronal excitability (*5–7*) and morphology (*8*), and possibly epileptogenesis (*9*) and in the neuronal conditioning phenomena implicated in learning and memory (*7, 10*).

Three major classes of neuronal VDCCs, L, N [both designated high voltage–activated (HVA)], and T [designated as low volt-

Department of Physiology and Molecular Biophysics, Baylor College of Medicine, Houston, TX 77030.

*To whom correspondence should be addressed.

age–activated (LVA)] are expressed and coexist in sensory and hippocampal neurons (*11–13*). However, only in a few cases (*14*) have electrophysiological methods shown how VDCCs are distributed over the nerve cell surface.

With appropriate probes, optical methods can provide detailed maps of ion channel distribution on living cells, in regions where access to patch pipettes is problematic (*15*). Such methods are also useful in developmental studies where successive noninvasive images are required. Results with Ca^{2+}-sensitive fluorescent dyes suggest a widespread distribution of intracellular Ca^{2+}, often concentrated into local hotspots on the growth cones, neurites, and cell bodies of stimulated neurons (*2, 16*).

A specific probe for neuronal N and L VDCCs, ω-conotoxin (ω-CgTx), has become available (*17*) and we now report on the distribution and mobility of VDCCs on cultured neurons from the hippocampal CA1 subfield with biologically active fluorescent and biotinylated derivatives of ω-CgTx and microscopic imaging methods.

Tetramethylrhodamine (TmRhd)–ω-CgTx and biotin–ω-CgTx were prepared by acylating ω-CgTx with the succinimidyl ester of 5(6)carboxytetramethyl-rhodamine or D-biotin, respectively. The modified derivatives were purified by reversed-phase high-performance liquid chromatography (HPLC) (Fig. 1A), and the monomodified derivatives were tested by equilibrium binding (*18*) (Fig. 1B). The dissociation constant (K_d) values for monomodified TmRhd–ω-CgTx and biotin–ω-CgTx conjugates were 10 n*M* and 20 n*M*, respectively, whereas the K_d for the native ω-CgTx was 0.6 n*M* (Fig. 1B).

The ω-CgTx derivatives also retained their biological activities. In whole-cell current measurements, TmRhd–ω-CgTx and biotin–ω-CgTx reduced voltage-dependent Ca^{2+} currents in hippocampal cells by 63 ± 8% (SD, n = 5) and 55 ± 10% (SD, n = 4), respectively, at concentrations of 25 n*M* (Fig. 1, C and D), values that correspond closely to the equilibrium binding constants.

The distribution of VDCCs on hippocampal CA1 neurons (*19*) was visualized by labeling neurons with biotin–ω-CgTx and TmRhd–ω-CgTx (*20*). Colloidal gold decoration of biotin ω-CgTx–labeled channels revealed VDCCs on cell bodies and processes (Fig. 2, A to C); because of the sensitivity and dichroic properties of colloidal gold, not only can single VDCCs be detected but also colors reflect cluster sizes such that the red regions, seen on cell bodies, represent regions of high VDCC density. On processes, labeling was either completely absent, interrupted by extensive bare regions, or terminated (Fig. 2B). These processes were identified as dendrites by double labeling with biotin–ω-CgTx and antibodies specific for microtubule-associated protein 2 (MAP-2), a protein localized to dendrites but not axons (*21*); all of the labeled VDCCs colocalized with MAP-2 immunofluorescence (Fig. 2, B and C). VDCC patches were also resolved on dendritic spines outlined by MAP-2 staining.

In order to explore VDCC distribution and mobility on living cells, we labeled hippocampal CA1 neurons with TmRhd–ω-CgTx (*22*). Digital fluorescence images of living neurons confirmed the presence of VDCCs on cell bodies (Fig. 2, D to I) and processes. Even in the absence of synaptic contact, multiple clusters of VDCCs were apparent against a sparse low density background distribution within a restricted area of the cell body (Fig. 2F, inset) (90 of 100 cells observed). However, on innervated neurons VDCCs were organized into a single cluster that coincided with the site of synaptic contact (Fig. 2, G to I) (four of five clearly identified innervated neurons). A steep gradient of VDCCs orginated from this site (Fig. 2I, inset).

The density profile of VDCCs was not due to local foldings of the membrane; neurons showed a homogenous distribu-

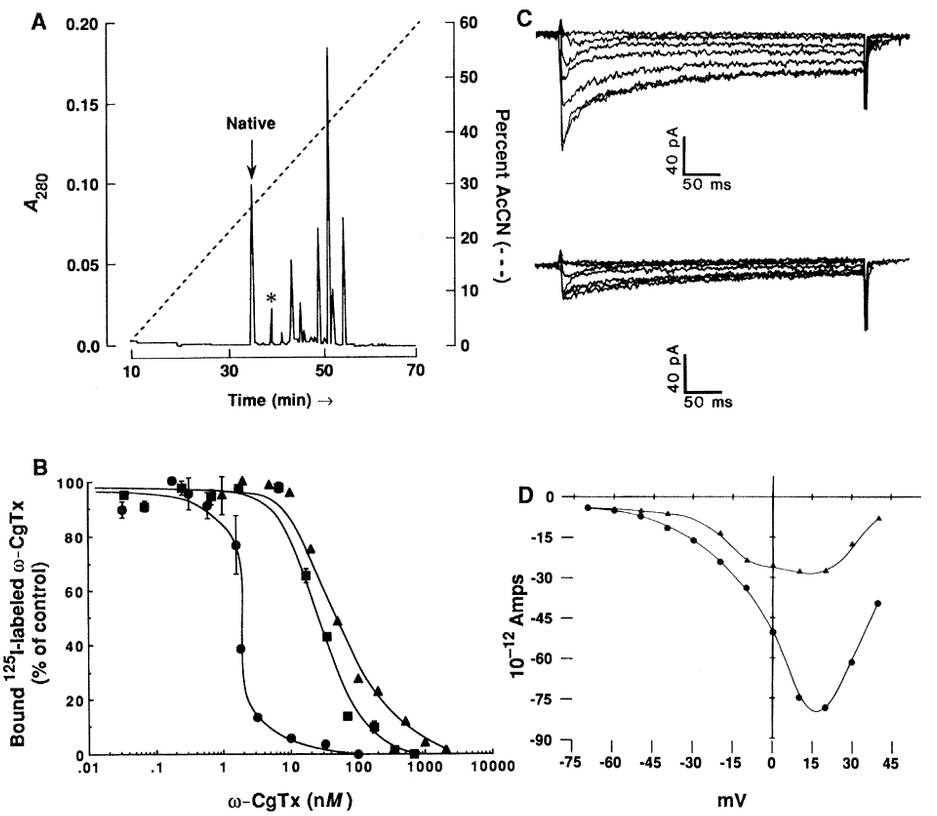

Fig. 1. Purification and characterization of ω-conotoxin (ω-CgTx) analogs. (**A**) Resolution of native ω-CgTx, TmRhd–ω-CgTx, and free dye products by reversed-phase HPLC. Native ω-CgTx was reacted at 25°C in the dark with the succinimidyl ester of 5(6)carboxytetramethyl-rhodamine (Molecular Probes) at a label to toxin ratio of 10:1 mol/mol in 500 μl of 100 m*M* $NaHCO_3$ (*p*H 9.5) for 1 hour, and the mixture was then applied to a Vydac C_{18} reversed-phase column. Reaction products were eluted with a 0 to 50% gradient of acetonitrile (AcCN) in 0.1% trifluoroacetic acid. Peaks were continuously monitored by measuring absorbance (*A*) at 226 or 280 nm. In some preparations, excess free dye was removed by dialysis before HPLC. The most potent monomodified TmRhd–ω-CgTx conjugate is indicated by an asterisk. (**B**) Displacement of ^{125}I-labeled ω-CgTx from rat brain synaptic membranes by native ω-CgTx (●), TmRhd–ω-CgTx (■), and biotin–ω-CgTx (▲). Values represent mean ± SD (n = 9). (**C** and **D**) Inhibition of voltage-dependent Ca^{2+} currents in hippocampal CA1 neurons by TmRhd–ω-CgTx. The membrane potential was held at −80 mV. Depolarizing voltage steps were applied to the cell in 10-mV increments. (C, top trace) Control currents were elicited at voltage steps to the potentials shown in (D). (C, bottom trace) The same voltages were applied immediately after a 30-s perfusion of the cell with 25 n*M* TmRhd–ω-CgTx. (D) The peak current-voltage relation before (●) and after (▲) addition of 25 n*M* TmRhd–ω-CgTx. Calcium currents were measured with the tight seal patch technique for whole-cell recording. The bath solution contained 125 m*M* tetraethylammonium chloride, 5.4 m*M* KCl, 2 m*M* $CaCl_2$, 10 m*M* glucose, 10 m*M* Hepes, and 5 m*M* 4-aminopyridine (*p*H 7.3). The pipette solution contained 124 m*M* CsCl, 11 m*M* EGTA, 1 m*M* $CaCl_2$, 2 m*M* $MgCl_2$, and 10 m*M* Hepes (*p*H 7.2). The TmRhd–ω-CgTx was diluted in the bath solution and applied to the cell by pressure application from a pipette placed approximately 20 μm from the cell.

tion of both TmRhd-succinyl–concanavalin A and TmRhd-phosphatidylethanolamine over the cell body surface (*23*). Images obtained with TmRhd–ω-CgTx and biotin–ω-CgTx were due to specific interactions; in the presence of saturating concentrations of native ω-CgTx, labeling was reduced by more than 80% over all parts of the neuron (*24*).

Some of the hippocampal neurons (approximately 10%), particularly those showing pyramidal-like morphology, were not labeled with either TmRhd–ω-CgTx or biotin–ω-CgTx (Fig. 2B, open arrow). Under the same solution and electrophysiological conditions, we did not find Ca^{2+} currents in these neurons, although these cells were typical of CA1 hippocampal neurons in other respects such as input resistance (>2 Gohm at −60 mV), expression of outward rectifying channels (*25*), morphology, MAP-2 expression, and labeling by Na^+ channel or γ-aminobutyric acid (GABA)–benzodiazepine receptor probes (*26*).

Using fluorescence photobleach recovery microscopy, we measured the lateral mobility of TmRhd–ω-CgTx–labeled VDCCs at several locations on the neuron (*27*). Even in the absence of synaptic contact, 70% of the VDCCs on the cell body were immobile, with diffusion coefficients (D) of $\leq 10^{-12}$ cm^2/s (Fig. 3); 30% of the VDCCs moved at rates of $(1.1 \pm 0.5) \times 10^{-10}$ cm^2/s (SD, $n = 94$), a value common for most membrane proteins. The size of the mobile fraction varied slightly with the density of the VDCC patch; in patches of lower density, 50 ± 7% of the channels were mobile and moved at rates 30 times faster [$D = (3.7 \pm 0.6) \times 10^{-9}$ cm^2/s (SD, $n = 18$)] than those found in hotspots. Photobleaching on dendrites (Fig. 3) showed that greater than 85% of the VDCCs were immobile [$D \leq 10^{-12}$ cm^2/s ($n = 56$)]. However, as on cell bodies, we consistently found that 15% of the VDCCs were rapidly mobile with lateral diffusion rates that were high for membrane proteins [$D = (8.6 \pm 0.5) \times 10^{-10}$ cm^2/s (SD, $n = 56$)], and close to those values for unrestricted free diffusion. Measurements of the lateral mobility of TmRhd-succinyl–concanavalin A receptors [$D = (3.0 \pm 0.7) \times 10^{-10}$ cm^2/s, 65 ± 8% mobile (SD, $n = 13$)], or TmRhd-phosphatidylethanolamine [$D = (8.3 \pm 0.4) \times 10^{-9}$ cm^2/s, 89 ± 9% mobile (SD, $n = 14$)] were similar in every region of the neuron tested. The different rates of mobility of VDCCs and concanavalin A receptors indicate that most of the VDCCs undergo greater retarding influences than those that are usually experienced by membrane proteins.

Our results suggest that the distribution and mobility of VDCCs has some measure of molecular specificity, since voltage-dependent Na^+ channels are sparsely distribut-

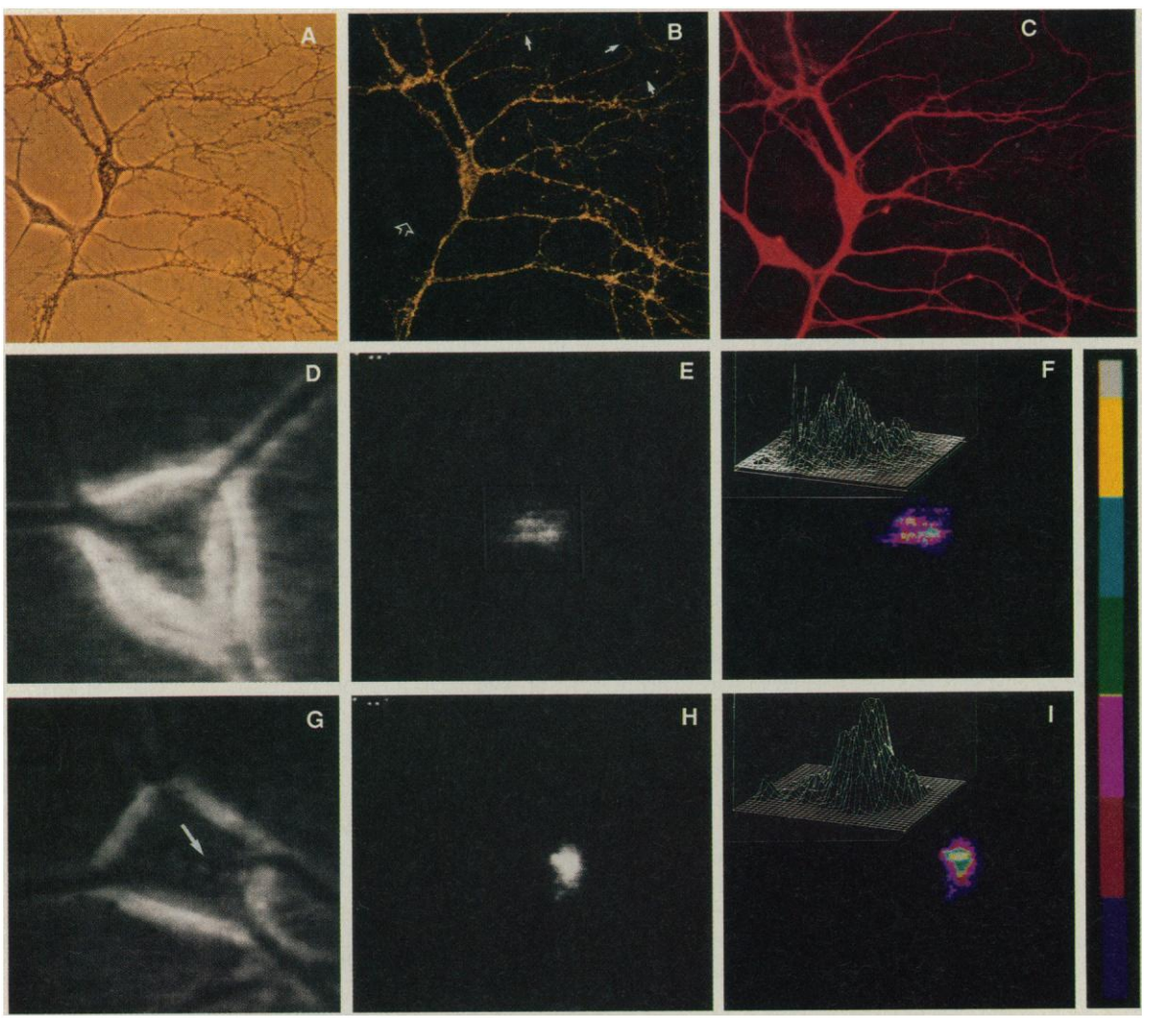

Fig. 2. Distribution of voltage-dependent Ca^{2+} channels on hippocampal CA1 neurons. (**A** to **C**) Hippocampal CA1 neurons were labeled with biotin–ω-CgTx and antibodies to MAP-2 protein (specific for dendrites) and viewed with phase-contrast (A), circular dityndallism (B), and epifluorescence optics (C). Circular dityndallism microscopy (B) shows the metallic deposits that correspond to single Ca^{2+} channels labeled with biotin–ω-CgTx and decorated with colloidal gold. In (C), cell bodies and dendritic processes of the neurons in (B) are outlined by MAP-2 immunofluorescence. Within this field is a neuron that is detected by antibodies to MAP-2 but not by biotin–ω-CgTx (open arrow). On neurons labeled with biotin–ω-CgTx, closed arrows denote bare or unlabeled regions of the dendrites where channels are absent. (**D** to **I**) Representative digital fluorescence images of living CA1 hippocampal neurons labeled by TmRhd–ω-CgTx. (D) and (G) are video images recorded with phase-contrast optics. (D) to (F) are images from a noninnervated hippocampal CA1 neuron and (G) to (I) of a hippocampal CA1 neuron that is innervated (G, arrow) from an adjacent cell. (E) and (H) are fluorescence images of the distribution of Ca^{2+} channels labeled with TmRhd–ω-CgTx and are the same field as in (D) and (G), respectively. (F) and (I) are representations of the fluorescence images in (E) and (H), respectively, with the grey levels displayed in color. The color scale corresponding to the grey level intensities (from levels 32 to 256) is shown at the right, with white representing the highest intensity. The insets in (F) and (I) show the intensity profiles of VDCC distribution over areas of 70 μm^2 and 50 μm^2, respectively.

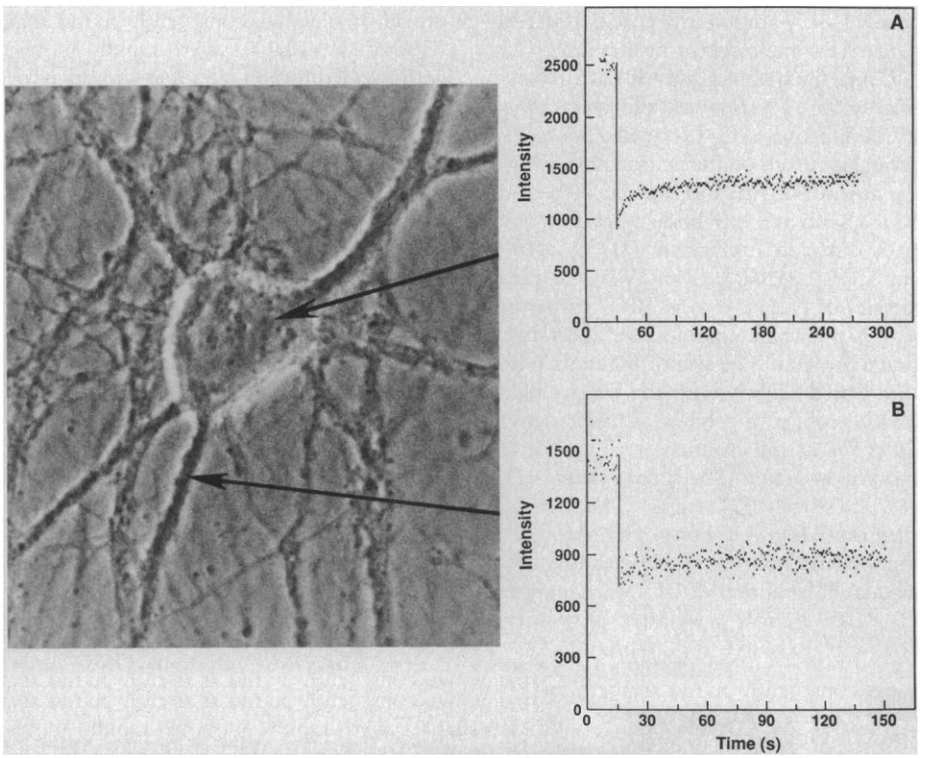

Fig. 3. Lateral mobility of voltage-dependent Ca^{2+} channels on hippocampal CA1 neurons. Fluorescence photobleach recovery (FPR) curves for Ca^{2+} channels labeled with TmRhd–ω-CgTx on a CA1 neuron (14 days in culture). FPR curves were obtained at the cell body (**A**) or the dendrite (**B**) at the indicated locations.

ed and very mobile on neuron cell bodies [$D = (1.8 \pm 0.4) \times 10^{-9}$ cm^2/s, 98 ± 5% mobile (SD, $n = 8$)] but segregated and immobilized at high density at specialized sites along the axon (*28*), whereas GABA-benzodiazepine receptors are localized and immobilized [$D \leq 10^{-12}$ cm^2/s ($n = 6$)] on neuronal cell bodies (*29*). The segregation and clustering of VDCCs on cell bodies and dendrites of hippocampal neurons is consistent with (i) inferences from electrophysiological studies showing that Ca^{2+} conductances are concentrated at foci of high sensitivity (*2, 11–13*), (ii) the variability in the number of channels in a given patch in cell-attached patch recordings (*2, 12*), (iii) intradendritic recordings showing large action potentials (*30*), and (iv) the mapping of Ca^{2+} signals with voltage- and Ca^{2+}-sensitive dyes (*31*).

The forces that limit the mobility of VDCCs are likely to contribute to their regional localization. The asymmetric distribution of VDCCs could arise by surface or intradendritic transport during neuronal growth (*32*) or by selective dendritic protein synthesis or transport of mRNA encoding VDCCs (*33*). The VDCCs could be confined to these regions by an intracellular barrier limiting movement between neighboring regions or through direct interactions with the cytoskeleton. Since other proteins and lipids can diffuse freely within dendrites or cell bodies or between these regions, a barrier that would confine VDCCs would have to be selective. A more plausible alternative would be an association of specific cytoskeletal proteins with VDCCs in each neuronal compartment. The localization and immobilization of Na^+ channels on axons, for example, is controlled through their association with axonal forms of ankyrin and spectrin (*34*). Indeed, the development of polarity in hippocampal neurons is accompanied by the asymmetric deposition of cytoskeletal proteins (*35*). Whereas cytoskeletal interactions may be responsible for immobilizing VDCCs, the recruitment of the mobile class of VDCCs to specific sites could confer additional plasticity to the neuron (*7*) and could greatly expand the neuron's ability to orchestrate and regulate Ca^{2+} signaling.

REFERENCES AND NOTES

1. R. J. Miller, *Science* **235**, 46 (1987); S. Hagiwara and L. Byerly, *Trends Neurosci.* **6**, 189 (1983).
2. D. Lipscombe *et al.*, *Proc. Natl. Acad. Sci. U.S.A.* **85**, 2398 (1988); S. R. Bolsover and I. Spector, *J. Neurosci.* **6**, 1934 (1986).
3. G. J. Augustine, M. P. Charlton, S. J. Smith, *Annu. Rev. Neurosci.* **10**, 633 (1987); R. S. Zucker and A. L. Fogelson, *Proc. Natl. Acad. Sci. U.S.A.* **83**, 3032 (1986); L. D. Hirning *et al.*, *Science* **239**, 57 (1988).
4. S. G. Miller and M. B. Kennedy, *Cell* **44**, 861 (1986); R. Siman, M. Baudry, G. Lynch, *Proc. Natl. Acad. Sci. U.S.A.* **81**, 3572 (1984).
5. R. Llinás and M. Sugimori, *J. Physiol. (London)* **305**, 197 (1980); R. K. S. Wong, D. A. Prince, A. I. Basbaum, *Proc. Natl. Acad. Sci. U.S.A.* **76**, 986 (1979); P. A. Schwartzkroin and M. Slawsky, *Brain Res.* **135**, 157 (1977).
6. H. Jahnsen and R. Llinás, *J. Physiol. (London)* **349**, 227 (1984); R. Llinás and Y. Yarom, *ibid.* **315**, 569 (1981); K. Kuba, *ibid.* **298**, 251 (1980).
7. E. Gamble and C. Koch, *Science* **236**, 1311 (1987); I. Segev and W. Rall, *J. Neurophysiol.* **60**, 499 (1988).
8. S. A. Lipton, *Neurosci. Lett.* **82**, 21 (1987); L. Anglister, I. C. Farbar, A. Shahar, A. Grinvald, *Dev. Biol.* **94**, 351 (1982); M. P. Mattson, A. Taylor-Hunter, S. B. Kater, *J. Neurosci.* **8**, 1704 (1988).
9. U. Heinemann and B. Hamon, *Exp. Brain Res.* **65**, 1 (1986); R. K. S. Wong and D. A. Prince, *Brain Res.* **159**, 385 (1978).
10. J. C. Eccles, *Neuroscience* **10**, 1071 (1983); G. Lynch, J. Larson, S. Kelso, G. Barrionuevo, F. Schottler, *Nature* **305**, 719 (1983).
11. E. Carbone and H. D. Lux, *J. Physiol. (London)* **386**, 571 (1987); S. A. Fedulova, P. G. Kostyuk, N. S. Veselovsky, *ibid.* **359**, 431 (1985).
12. A. P. Fox, M. C. Nowycky, R. W. Tsien, *ibid.* **394**, 173 (1987).
13. Y. Yaari, B. Hamon, H. D. Lux, *Science* **235**, 680 (1987).
14. S. Thompson and J. Coombs, *J. Neurosci.* **8**, 1929 (1988).
15. R. Y. Tsien, in *Optical Methods in Cell Physiology*, P. De Weer and B. M. Salzberg, Eds. (Wiley, New York, 1986), pp. 327–345; K. J. Angelides, in *Ion Channels*, T. Narahashi, Ed. (Plenum, New York, 1988), vol. 1, pp. 1–54; W. Almers and E. Neher, *FEBS Lett.* **192**, 13 (1985); S. M. Baylor and S. Hollingsworth, *J. Physiol. (London)* **403**, 151 (1988).
16. I. J. Reynolds *et al.*, *Proc. Natl. Acad. Sci. U.S.A.* **83**, 8804 (1986); J. A. Connor, *ibid.*, p. 6179.
17. W. R. Gray, B. M. Olivera, L. J. Cruz, *Annu. Rev. Biochem.* **57**, 665 (1988); L. M. Kerr and D. C. Yoshikami, *Nature* **308**, 282 (1984).
18. L. J. Cruz, D. S. Johnson, B. M. Olivera, *Biochemistry* **26**, 820 (1987); The K_d values were calculated from the experimentally determined $K_{0.5}$ [Y. C. Cheng and W. Prusoff, *Biochem. Pharm.* **22**, 2099 (1973)].
19. Hippocampal cultures were prepared as described [G. A. Banker and W. M. Cowan, *Brain Res.* **126**, 397 (1977)]. Cells were plated at a density of 2000 to 5000 per dish on polylysine-coated cover slips. After 4 days in culture, glial cell proliferation was suppressed by the addition of β-cytosine arabinoside (5 μ*M*) for 48 hours.
20. Hippocampal neurons were labeled with 500 n*M* biotin–ω-CgTx in medium A [Modified Eagle's Medium containing 5 m*M* Hepes-NaOH (*p*H 7.5) and 76 m*M* glucose]. After 45 min at 20°C, the cells were washed in medium A. Biotin–ω-CgTx was then decorated with colloidal gold by incubating the cells with streptavidin-gold (15-nm particle size) (Janssen Life Sciences) for 30 min. Cells were washed and fixed with 0.25% glutaraldehyde in 0.1*M* sodium cacodylate and 5 m*M* $CaCl_2$ (*p*H 7.4). Gold particle distribution was enhanced by silver intensification (Intense II kit, Janssen Life Sciences). Colloidal gold–decorated labeled channels were viewed by bright-field or circular dityndallism microscopy. In double-labeling experiments hippocampal neurons were fixed with methanol at −20°C for 20 min, rinsed in phosphate-buffered saline (PBS), and preincubated in 10% goat serum in PBS. Cells were exposed to antibody to MAP-2 (1:100 dilution) overnight at 4°C. The cultures were rinsed in 10% goat serum in PBS and incubated with rhodamine-labeled goat antibody to rabbit immunoglobulin G (IgG) (Kirkegaard and Perry Labs) for 2 hours at 25°C. Cells were mounted in Mowiol and immunofluorescence micrographs were recorded with a Zeiss Axiophot microscope. Control samples were treated identically, except either primary or secondary antibodies (or both) were omitted.
21. A. Cacéres, G. A. Banker, L. I. Binder, *J. Neurosci.*

6, 714 (1986); A. Cacéres, G. A. Banker, O. Steward, L. I. Binder, M. Payne, *Dev. Brain Res.* **13**, 314 (1984); P. De Camilli, P. E. Miller, F. Navone, W. E. Theurkauf, R. B. Vallee, *Neuroscience* **11**, 819 (1984); C. G. Dotti, G. A. Banker, L. I. Binder, *ibid.* **23**, 121 (1987).
22. Hippocampal neurons were labeled with 20 n*M* TmRhd–ω-CgTx in medium A (*20*). After 45 min at 21°C the cells were washed with medium A. Sequential phase and fluorescence images of the same field were obtained on-line with a Hamamatsu Photonics VIM camera mounted onto a Zeiss Photomicroscope III and through a ×63 water-immersion objective with a numerical aperture of 1.2. The 514-nm line of an attenuated and dispersed argon laser beam served as the illumination source for fluorescence images. Because of the low emission from fluorescence images, the intensifier of the camera was operated in the photon counting mode. Image sets were collected in real time and were either analyzed on-line or stored on videotape and later photographed.
23. O. T. Jones *et al.*, unpublished observations.
24. In addition, biotin–ω-CgTx and TmRhd–ω-CgTx label the same site; labeling of neurons with biotin–ω-CgTx was completely blocked by 200 n*M* TmRhd–ω-CgTx. Therefore, the more widespread channel distribution seen with biotin–ω-CgTx compared to TmRhd–ω-CgTx is due to technical aspects of the visualization, such as limited dynamic range and resolution of the camera, the small diameter of the dendrites relative to the imaging pixel size [K. R. Spring and R. J. Lowy, in *Methods in Cell Biology; Fluorescence Microscopy of Living Cells in Culture*, Y.-L. Wang and D. L. Taylor, Eds. (Academic Press, New York, 1989), vol. 29, pp. 269–289; P. J. Sammak and G. G. Borisy, *Nature* **332**, 724 (1988)] and the amplification and sensitivity of detection afforded by silver enhanced–colloidal gold and circular dityndallism microscopy [M. Hoefsmit, C. Korn, N. Blijlever, J. S. Ploem, *J. Microscopy* **143**, 161 (1986); M. De Waele, W. Renmans, E. Segers, K. Jochmans, B. Van Camp, *J. Histochem. Cytochem.* **36**, 679 (1988); S. Inoúe, A. S. Bajer, J. Mole-Bajer, *J. Cell Biol.* **91**, 321a (1981)], rather than differences in specificities of the two probes.
25. D. L. Kunze, unpublished observations.
26. K. J. Angelides, unpublished observations.
27. Fluorescence photobleach recovery measurements were made with the instrument described (*28*). The diffusion coefficient (*D*) and the mobile fraction (*f*) was determined by curve-fitting procedures (*28*). Incomplete recovery was interpreted to indicate immobility ($D \leq 3 \times 10^{-12}$ cm^2/s) of a fraction of labeled channels on the time scale of the experiment.
28. K. J. Angelides, L. W. Elmer, D. Loftus, E. Elson, *J. Cell Biol.* **106**, 1911 (1988).
29. J. L. Velazquez, C. L. Thompson, E. M. Barnes, K. J. Angelides, *J. Neurosci.*, in press.
30. L. M. Masukawa and D. A. Prince, *ibid.* **4**, 217 (1984); C. D. Woody, E. Gruen, K. McCarley, *J. Neurophysiol.* **51**, 925 (1984); R. Llinás and M. Sugimori, *J. Physiol. (London)* **305**, 171 (1980).
31. W. N. Ross and R. Werman, *J. Physiol. (London)* **389**, 319 (1987); D. W. Tank, M. Sugimori, J. A. Connor, R. R. Llinás, *Science* **242**, 773 (1988).
32. R. K. Small, M. Blank, R. Ghez, K. H. Pfenninger, *J. Cell Biol.* **98**, 1434 (1984).
33. L. Davis, G. A. Banker, O. Steward, *Nature* **330**, 477 (1987); C. C. Garner, R. P. Tucker, A. Matus, *ibid.* **336**, 674 (1988).
34. Y. Srinivasan, L. Elmer, J. Davis, V. Bennett, K. J. Angelides, *ibid.* **333**, 177 (1988).
35. C. G. Dotti, C. A. Sullivan, G. A. Banker, *J. Neurosci.* **8**, 1454 (1988).
36. We gratefully acknowledge the assistance of G. Schuster in providing the hippocampal neurons. Antibodies to MAP-2 were a gift from R. Vallee. We are indebted to J. Kirkpatrick for the use of image analysis equipment and J. Heath for the use of the Zeiss Axiophot fluorescence microscope. This work was supported by grant NS24606 and a Research Career Development Award NS01218 to K.J.A. and grant NS23573 to D.L.K. and with funds from the Biomedical Support Research Grant to O.T.J.

7 December 1988; accepted 30 March 1989

The Neuronal Growth-Associated Protein GAP-43 Induces Filopodia in Non-Neuronal Cells

MAURICIO X. ZUBER, DANIEL W. GOODMAN, LARRY R. KARNS,* MARK C. FISHMAN

The neuron-specific protein GAP-43 is associated with the membrane of the nerve growth cone and thus may be important to the activity of this distinctive neuronal structure. Transient transfection of COS and NIH 3T3 cells with appropriate vectors resulted in expression of GAP-43 in these non-neuronal cells; as in neurons, transfected GAP-43 associated with the membrane. In addition, many long fine filopodial processes extended from the periphery of such transfected cells. Stable CHO cell lines expressing GAP-43 also exhibited processes that were more numerous, far longer, and more complex than those of CHO cell lines not transfected or transfected with control plasmids. Thus GAP-43 may directly contribute to growth cone activity by regulating cell membrane structure and enhancing extension of filopodial processes.

THE PROTEIN GAP-43 IS NEURON-specific and is associated with the membrane of growth cones. Although its specific cellular function is unknown, it has been proposed to be important to growth cone function during development and to the remodeling of neuronal connections in the adult. Evidence in support of such a role for GAP-43 includes (i) the coincident expression of GAP-43 with periods of axonal elongation and regeneration in both mammals and amphibia, and with neurite growth in PC12 cells (*1, 2*); (ii) transport to, and enrichment of, the protein on membranes of the growth cone (*3*); (iii) persistence of GAP-43 expression in regions of the adult central nervous system believed to be important in learning and memory (*4, 5*); and (iv) changes in the phosphorylation state of GAP-43 in association with long-term potentiation (*6*). This protein has also been postulated to play a role in signal transduction at the membrane by binding calmodulin (*7*) and regulating the synthesis of phosphatidylinositol 4,5-bisphosphate (*8*).

To test the hypothesis that GAP-43 regulates growth cone function, we introduced expression vectors encoding rat GAP-43 into non-neuronal cells. In such cells the function of GAP-43 might be more easily

Developmental Biology Laboratory, Massachusetts General Hospital Cancer Center, and the Howard Hughes Medical Institute, Massachusetts General Hospital, Boston, MA 02114, and Harvard Medical School, Boston, MA 02115.

*Present address: Cardiovascular Research Institute, University of California, San Francisco, San Francisco, CA 94121.

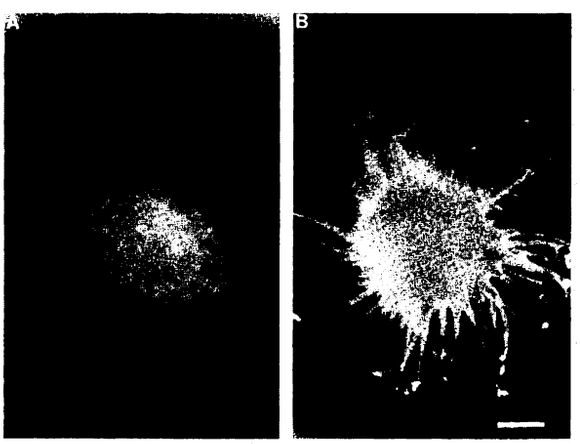

Fig. 1. Immunofluorescence of COS-7 cells transfected with (**A**) CD8 or (**B**) GAP-43. Mock-transfected cells or cells transfected with CD8 were generally round after plating, although some had a few short processes. Process extension, as from the cell in (B), was only seen in cells expressing large amounts of GAP-43, although there was a spectrum of shapes for those cells with GAP-43; some cells had smaller, longer, or fewer processes than the cell shown here, and some cells did not appear different from control cells. Bar, 10 μm. The expression vectors contained the cytomegalovirus promoter with either rat GAP-43 or CD8. The GAP-43 expression plasmid (CDM8-GAP) was constructed by inserting rat GAP-43 coding sequences (*14*) at the Xba I site of the plasmid pCDM8 (*15*). This plasmid contains the cytomegalovirus promoter, the simian virus 40 polyadenylation signal and origin of replication, and the polyoma virus origin of replication. The expression vector encoding CD8 was of similar construction (*16*). Cells were transfected by DEAE-dextran (*17*). After 48 hours the cells were passed by trypsinization and plated on cover slips coated with poly-D-lysine (0.1 μg/μl). The cells were fixed in 3.7% formaldehyde 1 hour after plating. Cover slips were incubated for 1 hour in 1% normal goat serum in phosphate-buffered saline and then incubated with either rabbit antibody to GAP-43 (*5*) or the monoclonal antibody OKT8 to CD8 (American Type Culture Collection). Appropriate secondary goat antibodies labeled with fluorescein isothiocyanate (Cooper Biomedical) were used to detect immune complexes.